Bull. Mater. Sci., Vol. 36, No. 1, February 2013, pp. 1–7. © Indian Academy of Sciences.

Carbon nanotubes purification constrains due to large Fe–Ni/Al_2O_3 catalyst particles encapsulation

GORAN BOSKOVIC*, SANJA RATKOVIC, ERNE KISS and OLGA GESZTI†
Faculty of Technology, University of Novi Sad, Bul. cara Lazara 1, 21000 Novi Sad Serbia
†Research Institute for Technical Physics and Materials Science, P.O. Box 49, Budapest H-1525, Hungary

MS received 10 August 2011; revised 22 September 2011

Abstract. **Purification efficiency of carbon nanotubes (CNTs) by the method of chemical oxidation was considered as a function of position and size of catalyst remains and consequently of the tubes morphology. Oxidation of CNTs by means of both HNO_3 and NaOH treatment efficiently removes small catalyst particles embedded in the tubes top, following "tip-mode" CNTs growth mechanism. Destructive character of the purification can be assumed due to the resulting tiniest tube population increase as a consequence of their body tearing. However, limited purification efficiency was observed in the case of bigger metal particles with variable size and position in CNTs. Bigger particles occur on account of catalyst instability portrayed as small metal particles of active phase migration and merging. The formed agglomerates are not stable in the tubes hollow, but disintegrate leading to different sizes and position of metal particles in the tubes body. Consequently, CNT may be obtained with non-uniform thickness and morphology. The phenomenon is due to liquid-like behaviour of the active phase at reaction temperature (700 °C) which is higher than both Huttig and Tamman temperatures of applied metals. A mechanism is proposed assuming that an isolated bigger part of the mother particle stayed encapsulated inside the tube body inactive for further tube growth, while a smaller fragment of the collapsed particle resided at the tube top acting as a new-born active site. Owing to "replica effect" the tube further grows thinner following the size of the new active site. Consequently CNTs of irregular morphology occur as they resemble metal particles of various sizes following their disintegration.**

Keywords. **CNTs purification; catalyst Fe–Ni/Al_2O_3 particles encapsulation; active sites disintegration; irregular CNTs morphology.**

1. Introduction

Since their discovery (Iijima 1991), carbon nanotubes (CNTs) have become very promising material for many technological applications due to their unique structure and variety of possible application. CNTs produced by catalytic chemical vapour deposition (CCVD) method often contain impurities (amorphous carbon, graphite) which together with catalyst particles have to be removed during purification. Till now, there are many suggested purification methods which, in general, can be classified into three major methods: physical separation, gas-phase oxidation and liquid-phase oxidation (Montoro and Rosolen 2006). However, there is no unique purification procedure for fulfilling all the requirements set by the CNTs application fields. Besides, the purification procedure may be oriented to two different goals: to maintain the structure and crystallization degree of the tubes, or to modify their structure and create surface functional groups. Thus, Chen *et al* (2007) showed that the microwave digestion acidic procedure is an effective and fast method to clean the tubes and open their ends. This leads to the increase of the BET surface area, especially in the case of tubes with smaller diameters (10–20 nm). According to Monchelaho *et al* (2011), efficiency of multi-walled CNTs purification depends on acidic treatment conditions. Thus, the most harsh purification conditions (55% HNO_3 for 6 h) generated the roughest carbon surface and consequently decreased the tubes outer diameter. However, the treatment led to removal of all residual catalyst, while the metal particles observed within the tubes stayed encapsulated. In addition (Chen *et al* 2004), the metallic catalyst particle during tube growth may break into two parts. In the case of the "base-growth" model, the bottom part stays at the support and is responsible for further tube growth, while the top one is fully encapsulated and therefore inactive.

In our previous work high CNTs yield and selectivity due to optimal metal-support interaction (MSI) in Fe–Ni/Al_2O_3 catalyst has been discussed (Ratkovic *et al* 2011). In addition "tip-growth" mechanism of CNTs growth in CCVD using ethylene has been proposed. The aim of the present work is to study effects of purification of CNTs by means of chemical oxidation and correlation of its efficiency to morphology of both as-obtained and purified CNTs. It is assumed that tubes morphology, which is controlled by growing mechanism and catalyst stability, will govern the way of catalyst removal.

*Author for correspondence (boskovic@uns.ac.rs)

2. Experimental

2.1 *Catalyst synthesis*

Bimetallic Fe–Ni (2·5 wt% of each metal loading) catalyst has been prepared and tested before (Ratkovic *et al* 2011). Basically, coprecipitation of both metal hydroxides on commercial γ-Al_2O_3 powder suspended in water has been applied, following catalyst precursor washing, drying and calcination at 600 °C for 5 h.

2.2 *Carbon nanotubes synthesis and purification*

The CNTs growth was carried out by means of CCVD method using ethylene in a home-made reactor set up consisting of a horizontal oven and a system for diluted ethylene supply (Ratkovic *et al* 2011). The catalyst precursor powder (700 mg) was placed in the form of thin layer in a quartz boat located in the middle of the quartz reactor, with reaction temperature measured at the outer wall of the reactor. Preceding the C-nanotubes synthesis, the catalyst was *in situ* reduced in controlled hydrogen flow (110 ml/min) at 700 °C for 2 h. Subsequently the hydrogen was replaced by flow of 220 ml/min of ethylene/nitrogen mixture (1:1) and the synthesis was carried out at the same temperature for 1 h. After the system was cooled in N_2 flow to room temperature, the catalyst and accumulated C-containing material were discharged. The raw product was purified by means of sequential 6 h boiling with reflux, using 3M NaOH and HNO_3 solutions for removal of the catalyst active phase and support, respectively with intermediate sample washing. Finally, the purified carbon nanotubes were washed with distilled water and dried at 110 °C for 24 h.

2.3 *Characterization of as-grown and purified CNTs product*

Scanning (SEM JEOL JSM-6460LV) and transmission (Philips CM20 200 kV analytical microscope) electron microscopy with additional qualitative analysis by energy dispersive spectroscopy (EDS) were used for CNTs morphology characterization. Tubes diameters distribution before and after purification was done measuring of about 100 samples chosen from TEM images. CNTs textural characteristics were determined by means of low temperature N_2 adsorption/desorption (LTNA) method, using He as a carrier gas (micromeritics ASAP 2010). Specific surface area was calculated by BET equation, while mean pore diameter and pore volume were determined from adsorption part of the N_2 isotherm and calculated by Barrett–Joyner–Halenda (BJH) method (Barrett *et al* 1951). Pores were classified according to Brunauer–Deming–Deming–Teller method based on hysteresis loops of adsorption–desorption isotherms (Lowell *et al* 2004).

3. Results and discussion

SEM and TEM images of as-obtained carbon products are given in figures 1(a) and (b), respectively. Appearance of dense and homogeneously distributed CNTs covering the whole catalyst surface, shown in figure 1(a), is in line with high yield reported earlier (Ratkovic *et al* 2011). However, the image testifies to a highly twisted shape of as-grown CNTs which might indicate the presence of structural defects responsible for their emphasized bending (Hernadi *et al* 1996). As can be seen from TEM image (figure 1(b)), as-obtained CNTs are pretty unique with thickness varying mostly within 10–30 nm. However, a lot of dark patches are present indicating catalyst remains differing by their size as well as position inside the CNTs. Still "replica effect" may be assumed as a rule governing the tubes growth (Hernadi *et al* 1996; Louis *et al* 2005), as ranges of metal particle size mostly coinciding with tubes diameters. Analysis of the same structures by TEM covering larger shooting area (figure 2(a)) shows different scenario, however, like catalyst particles of different sizes with surroundings variously populated with CNTs. As proved by EDS shown in the box on the

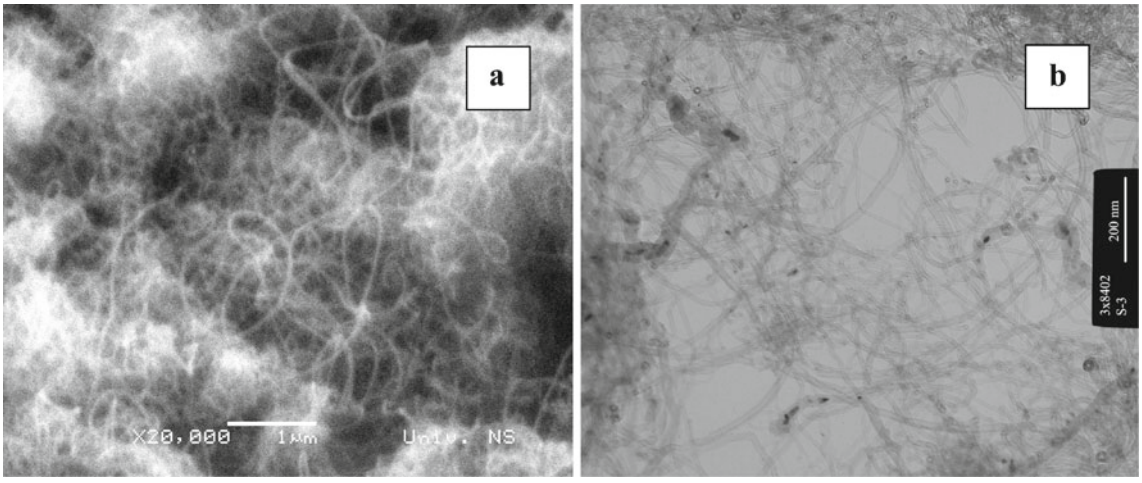

Figure 1. SEM (**a**) and TEM (**b**) images of as-obtained CNTs.

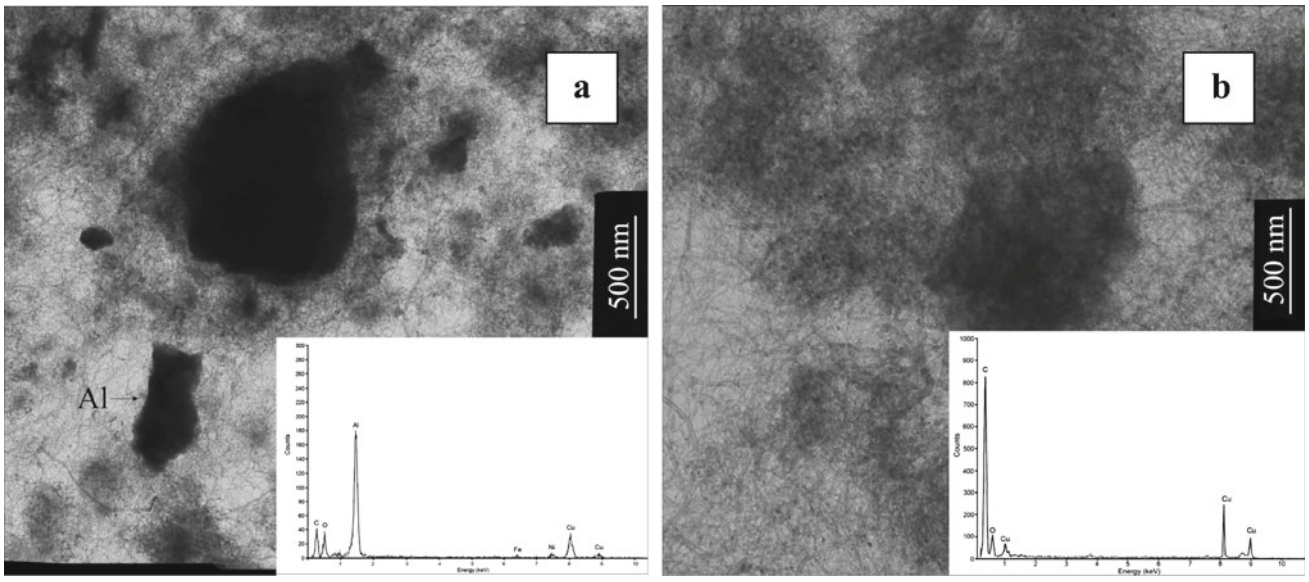

Figure 2. TEM images of as-obtained (**a**) and purified (**b**) CNTs and corresponding EDS data for qualitative analysis.

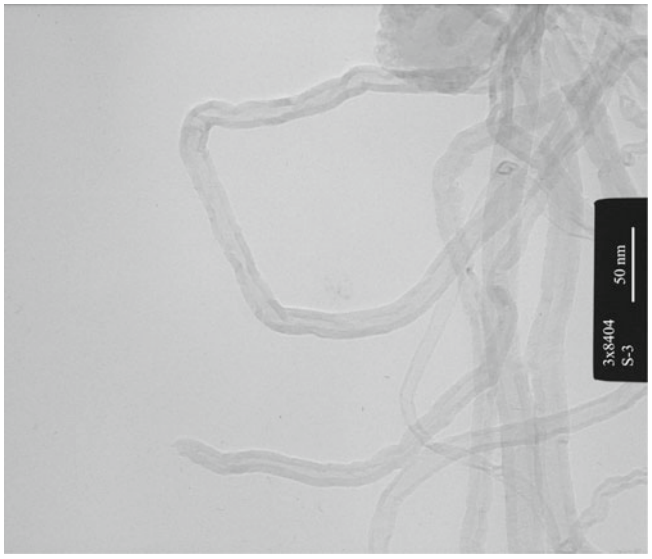

Figure 3. TEM image of purified CNTs.

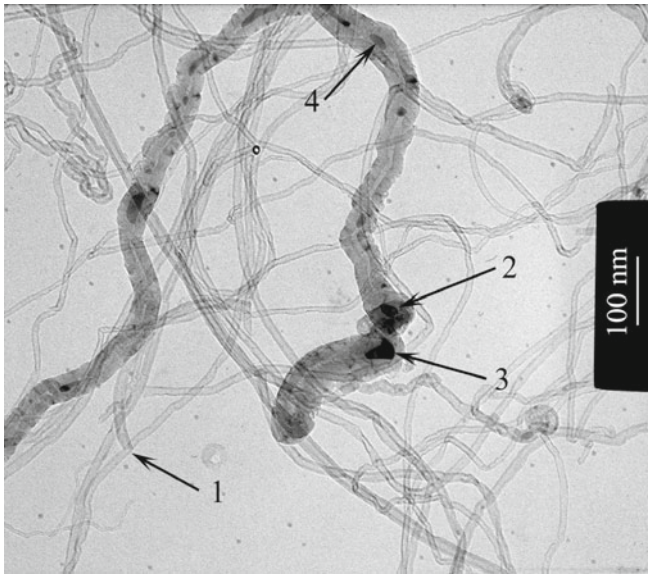

Figure 4. TEM image of thicker purified CNT with embedded metal particles which resisted purification procedure.

right-hand side of the same picture, mostly catalyst components can be identified (analysis of particle in the lower left side marked as Al), and only traces of C-containing product structures can be anticipated. This is in line with generally known requirement for high catalyst active-phase dispersion as a prerequisite for high yield of CNTs and their uniform size. Result of CNTs purification can be seen in figure 2(b); EDS analysis without any doubt proves that catalyst remains were efficiently removed from as-obtained CNTs by chemical oxidation method, as neither supports nor any metals comprising the bimetallic catalyst is present after purification (Cu, as the dominant element found next to C, comes from the sample holder used for the analysis).

A microscopic look taken after purification, given by TEM image in figure 3, witnesses nicely purified tubes of similar morphology. Their structure seems preserved, except for an open end of a single tube in the left-hand corner of the picture. As shown by figure 4, however, not all the tubes are characterized by the same low size diameter, as there are some of them which are much thicker. Besides, the purification is efficient only to those tubes that have catalyst particles easily available to oxidation agents, i.e. to those situated on the top of the CNTs. Namely, the point 1 marked in figure 4 indicates a thin tube with a cracked end as a probable spot from which a metal particle has been removed.

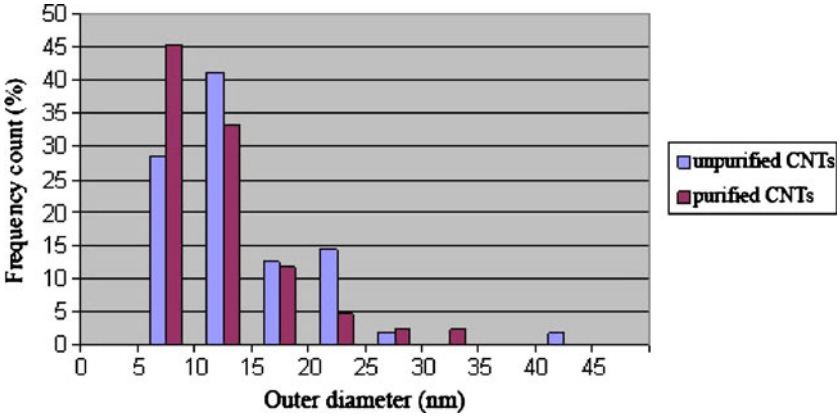

Figure 5. Distribution of CNTs as a function of their diameters before and after purification (based on measurements of about 100 samples chosen from TEM images).

Thus, opening ends of tubes with small diameter that have the "tip-growth" history precedes the catalyst particle leaching. Quite different behaviour is observed in the case of thicker tubes, having bigger metal particles which remained encapsulated yet after the oxidation treatment (positions 2, 3 and 4 in figure 4). The high resistance of these particles is associated with the body stability of thicker tubes relative to the slim ones, the latter performing easy opening of tips having thin walls. This may be associated with different oxidation tendencies between the C-structure building tips and bodies of the tubes (Son *et al* 2008), but also may be due to various numbers of C-layers forming the tubes wall of different thicknesses.

Results of a detailed statistical analysis of CNTs thickness shown in figure 5 prove that about 70% of the as-obtained CNTs have outer diameter between 5 and 15 nm. Knowing, however, that their corresponding inner diameter is roughly 2–6 nm smaller (depending on number of walls in a particular case), this can be used as an additional fact narrowing the actual size distribution of the catalyst active sites responsible for the CNTs growth. As presented by histogram given in figure 5, tubes diameter distribution confirms a destructive character of the applied refining method, since fraction of tiniest tubes having diameter 5–10 nm increased by about 17% upon the catalyst removal. In other words, next to tips opening necessary for the metal removal, cracking of tiniest tube bodies occurs and hence their population increases (figure 5).

Generally, mobility of catalyst metal particles towards interiors of growing CNTs is a function of specific degree of catalyst metal-support interaction. A week metal-support interaction (WMSI) has been known as the prerequisite for easy catalyst active phase extraction, followed by "tip-mode" as ruling growth mechanism of CNTs (Teo *et al* 2001). Occurrence of encapsulated catalyst particles of bigger size resisting tubes purification in a particular case (figure 4) must be connected to the catalyst quality. That is to say, non-uniform dispersion of active phase throughout the catalyst results in active sites of different sizes followed by CNTs of different thicknesses.

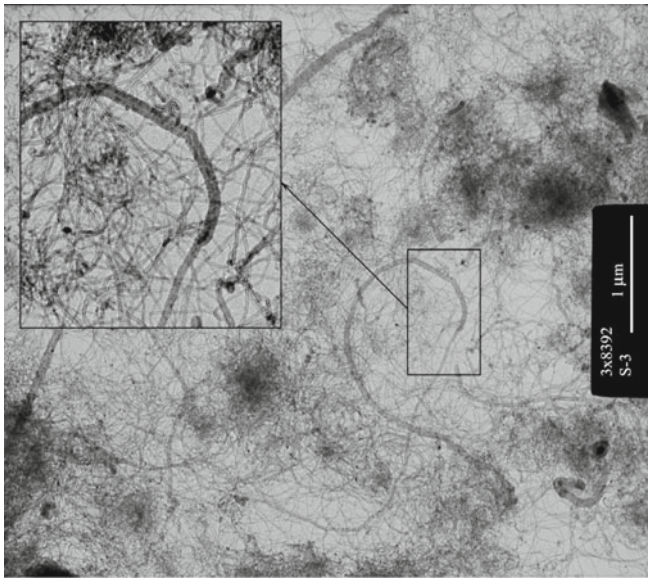

Figure 6. TEM image of tube with irregular diameter.

Liquid-like behaviour of active metal has been extensively used in catalysis to explain catalyst deactivation by sintering. It is manifested as metal particles migration and coalescence occurring at temperatures pretty lower than melting temperature of the metal (Boskovic and Baerns 2004). The cases of catalyst particle encapsulation in CNTs have been explained in the literature as following metal particles nucleation and coalescence (Ermakova *et al* 2001) due to quasi-liquid state of the metal at high temperature (Qian *et al* 2003; Gulino *et al* 2005). Recently, a model based on iron–carbide particle disintegration by carbon growing thereon, has been offered to explain the position of the metal which has been dragged into the hollow carbon tube (Ermakova and Ermakov 2002).

In line with the former, here applied reaction temperature higher than Tamman and Huttig temperatures of both Ni and Fe (Moulijn *et al* 2001) might have provided a suitable environment for such an easy-to-move metal particles to release from the catalyst surface by growing CNT.

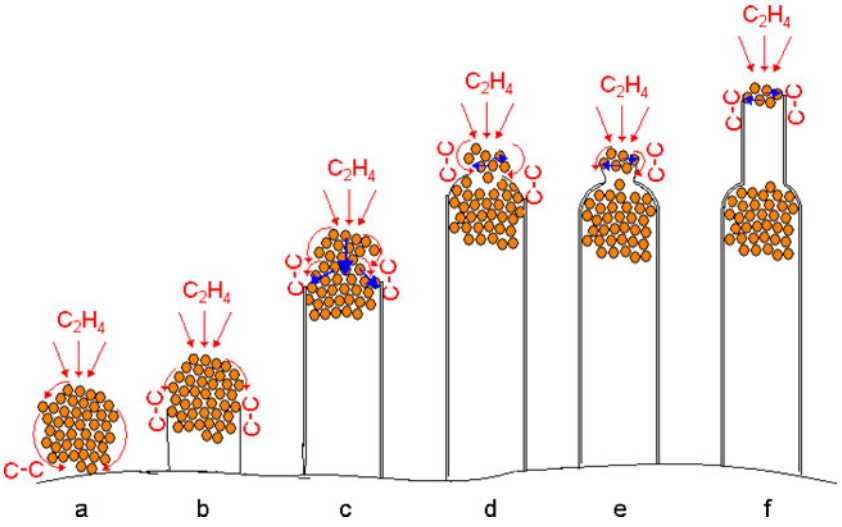

Figure 7. Model of tubes "tip-growth" comprising quasi-liquid metal particle disintegration preceding tube morphology change.

Table 1. Textural properties of CNTs and related catalyst.

	Calcined catalyst	As-obtained CNTs	Purified CNTs
BET ($m^2 \cdot g^{-1}$)	186·0	175·1	191·0
Average pore diameter[a] (nm)	5·6	13·8	15·9
Total pore volume[a] ($cm^3 \cdot g^{-1}$)	0·36	0·78	0·89

[a]Calculated based on desorption part of isotherm.

This scenario is preceded by WMSI established during the catalyst preparation and/or used to allow the small metal particles migration and coalescence to bigger structures, and is followed by (part of) big metal particles encapsulation inside the channel of growing carbon tube. TEM image given in figure 6 with a square showing a magnified picture of nanotube having irregular diameter is in line with the former explanation. This picture supports the idea of the catalyst active phase instability as determining factor of metal encapsulation by growing nanotubes, which in turn suffer morphological defects. Namely, as seen from the TEM image in figure 6, a metal particle which stays encapsulated in the tube is positioned at the same point where the tube diameter has been changed. The possible mechanism is explained by scheme given in figure 7. Dissociative chemisorption of C-feedstock is followed by C-atom diffusion on the surface of the large particle before being stabilized at the metal/support interface (Gohier *et al* 2008). Due to WMSI the tube starts to grow following "tip-growth" model, with the atomic cluster positioned on its top exposed for further carbon adsorption (a–b). Following tube growth stretching forces start to elongate the metallic cluster which is in a quasi-liquid state at 700 °C, while ethylene diffusion through the bulk of the metal particle occurs next to the diffusion over surface (c). Further stretching forces form a neck on the metal particle followed by carbon deposition at this point and formation of the first graphene layer that covers the upper part of the mother (bigger) metal particle (d). Extended formation of graphene layers isolates the mother particle which in turn becomes inactive; the tube with smaller diameter continues to grow following the size of the new-born active site on its top (e–f). The proposed mechanism of particle encapsulation slightly differs from one related to the "base-mode" of CNTs growth (Chen *et al* 2004), in which fragmented metal particle on the tube top becomes inactive, while the mother particle sitting at the catalyst support continues to act as active site for further tube growth.

Textural properties and pore size distribution profiles of related product before and after purification, as well as of the corresponding catalyst for comparison, are given in table 1 and figure 8, respectively. CNTs are characterized by very high specific surface area, as well as mesoporous structure resulting in much higher mean pores diameter and pore volume relative to the applied catalyst (table 1). In the case of as-obtained carbon material three-dimensional porous structure can be observed, with pores of about 5 nm diameter most probably belonging to the present catalyst (note that the pores of that diameter represent the entire porous structure of the catalyst sample) (figure 8). After successful catalyst removal, these pores disappear and both specific surface area and total pore volume of purified CNTs fairly

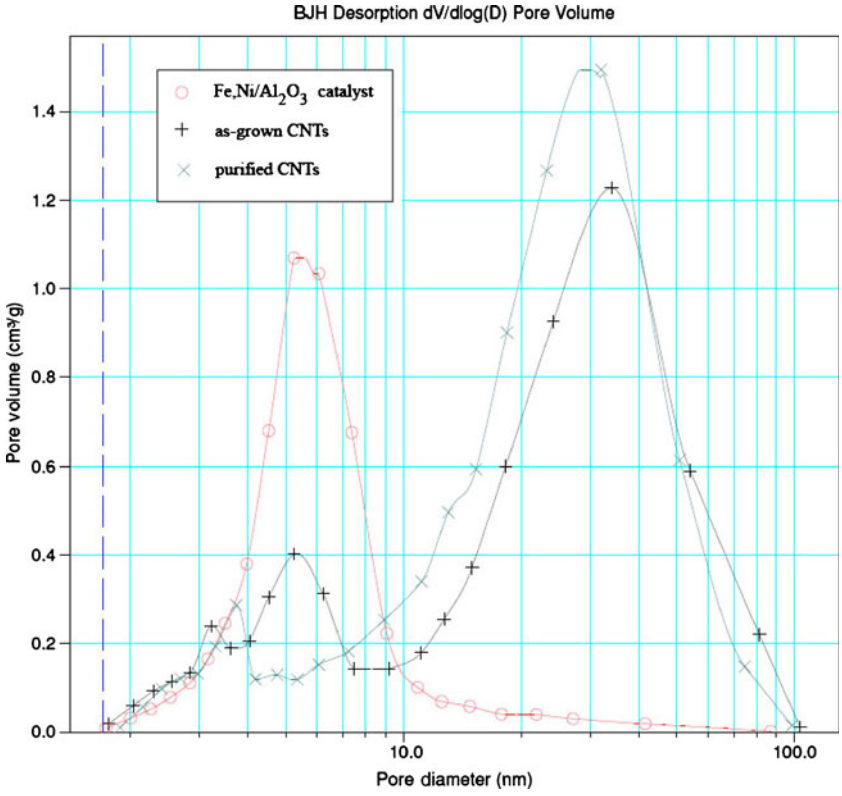

Figure 8. Pore size distribution of as-obtained CNTs, purified CNTs and related Fe–Ni/Al_2O_3 catalyst.

increase. Therefore, changing of CNTs texture upon purification can hardly be explained by tube ends opening, but rather by tubes body tearing increasing their population and tubes interstices. Indeed, as seen from figure 8, the stressing feature of this material is a dominating fraction of pores in the high meso-range diameter (30 nm and higher), considerably larger than the size of CNTs hollow observed in TEM images in figures 3 and 4. Obviously, the dominant mesopore structure of both as grown and purified CNTs comes not from their hollow interiors but from interstices originating along the tangled tubes. Adsorption/desorption isotherm hysteresis of CNTs, both unpurified and purified (not shown), differs significantly from that of the catalyst indicating presence of pores in the tubes which can be described as fractures (Lowell *et al* 2004). This pore structure makes CNTs promising material for various applications as adsorbents, or catalyst supports, in processes comprising reactants/products having high molecular weight.

4. Conclusions

Multi-walled CNTs obtained over bimetallic Fe–Ni/Al_2O_3 catalyst can be efficiently purified by liquid oxidation method. Basically, small particles sitting on the tube tops, responsible for "tip-growth" mode, are easily removed. On the other hand, metal particles of various sizes, encapsulated inside thicker nanotube bodies, are resistible to the applied purification treatment. Beside, diameters of these CNTs do not resemble the size of original metal particles acting as an active site due to catalyst particle disintegration during tube growth. The process of the active metal fragmentation occurs at reaction temperatures higher than Tamman or Huttig temperatures at which metal particles show quasi-liquid behaviour. Following the metal particle disintegration, the tube continues to grow, with its morphology resembling smaller diameter of emerged active site sitting at the tube top ("tip-growth" mechanism). A part of original big metal particle stays encapsulated inside the CNT channel inactive for further growth. The applied liquid oxidation has a destructive character, increasing the population of the most fragile tiniest tubes upon their bodies tearing. In turn, CNTs textural characteristics improve on account of the size of the tubes interstices in the meso-range, making a dominant contribution to porous structure.

Acknowledgement

This work was supported by the Ministry of Science and Technological Development of Serbia (project 172059).

References

Barrett E P, Joyner L G and Halenda P P 1951 *J. Am. Chem. Soc.* **73** 373

Boskovic G and Baerns M 2004 *Catalyst deactivation in basic principles of applied catalysis* (ed) M Baerns (Berlin: Springer) p. 479

Chen M, Yu H W, Chen J H and Koo H S 2007 *Diamond Relat. Mater.* **16** 1110

Chen X, Wang R, Xu J and Yu D 2004 *Micron* **35** 455

Ermakova M A and Ermakov D Y 2002 *Catal. Today* **77** 225

Ermakova M A, Ermakov D Y, Chuvilin A L and Kuvshinov G G 2001 *J. Catal.* **201** 183

Gohier A, Ewels C P, Minea T M and Djouadi M A 2008 *Carbon* **46** 1331

Gulino G, Vieira R, Amadou J, Nguyen P, Ledoux M J, Galvagno S, Centi G and Pham-Huu C 2005 *Appl. Catal. A* **279** 89

Hernadi K, Fonseca A, Nagy J B, Bernaerts D and Lucas A A 1996 *Carbon* **34** 1249

Iijima S 1991 *Nature* **354** 56

Louis B *et al* 2005 *Catal. Today* **102** 23

Lowell S, Shields J E, Thomas M A and Thommes M 2004 *Characterization of porous solids and powders: surface area, pore size and density* (Dordrecht/Boston/London: Kluwer Academic Publishers)

Monchelaho M A M, Xiong H, Moyo M, Jewell L L and Coville N J 2011 *J. Mol. Catal. A* **335** 189

Montoro L A and Rosolen J M 2006 *Carbon* **44** 3293

Moulijn J A, van Diepen A E and Kapteijn F 2001 *Appl. Catal. A* **212** 3

Qian W, Liu T, Wang Z, Yu H, Li Z, Wei F and Luo G 2003 *Carbon* **41** 2487

Ratkovic S, Vujicic Dj, Kiss E, Boskovic G and Geszti O 2011 *Mater. Chem. Phys.* **129** 398

Son S Y, Lee Y, Won S and Lee D H 2008 *Ind. Eng. Chem. Res.* **47** 2166

Teo K B K, Singh C, Chowalla M and Milne W I 2001 *Encyclopedia of nanoscience and nanotechnology* (USA: American Scientific Publishers)